ANALYTICAL SCIENCES FEBRUARY 2012, VOL. 28

Separation of Gold Nanoparticles with a Monolithic Silica Capillary Column in Liquid Chromatography

Siswoyo, Lee Wah LIM, and Toyohide TAKEUCHI†

Department of Chemistry, Faculty of Engineering, Gifu University, 1-1 Yanagido, Gifu 501–1193, Japan

A separation system for gold nanoparticles was developed using monolithic silica capillary columns with 50 μm i.d., which were prepared *via in-situ* sol-gel processes. Gold nanoparticles with five different average sizes were synthesized *via* reduction of tetrachloroauric acid ($HAuCl_4$) under different synthesis conditions, and were evaluated by UV-visible spectrophotometry, dynamic light scattering as well as transmission electron microscopy before they were separated using the developed system. The results showed that all of the gold nanoparticles had a certain size distribution, and the mean sizes obtained were 13, 17, 33, 43 and 61 nm, with σ = 2.5, 2.7, 5.2, 5.1 and 5.6 nm, respectively. Transmission electron microscopy showed that the samples with mean sizes of 13 and 17 nm were almost spherical, while larger samples were slightly non-uniform. The agglomeration of gold nanoparticles as the sample could be prevented by using a sodium dodecyl sulfate aqueous solution as the mobile phase, and gold nanoparticles were retained by adsorption on the silica surface. Separation with 8 mM sodium dodecyl sulfate as the eluent and a 1000-mm column was successful, and the separation of gold nanoparticles with 61 and 17 nm or 61 and 13 nm was demonstrated. The separation results obtained using a nonporous silica packed column as well as monolithic silica columns with or without mesopore growth were compared. It was found that separation using the mesopore-less monolithic column achieved better resolution. Through the use of a 2000-mm separation column, the mixtures of 61, 43, 17 nm and 61, 33, 13 nm could be separated.

(Received October 24, 2011; Accepted November 11, 2011; Published February 10, 2012)

Introduction

Gold nanoparticles have been studied for many years due to their physical characteristic, especially the optical characteristics related to size and shape.[1] The optical characteristics of gold nanoparticles are important because their absorption and emission of the wavelength are within the visible range of light. Due to this unique physical characteristic, gold nanoparticles have a broad range of application in catalyst,[2] biology,[3] optics,[4] and other areas of high technology. Faraday's gold sols, which were produced in the mid-nineteenth century, represent the first documented scientific investigation on the dispersion of fine gold particles.[5] More recently, new techniques as well as improvements to classical methods have made it possible to synthesize nanoparticles with controlled sizes, which has become important, and one of the most current topics. For example, gold nanoparticles with the size controlled can be potentially applied in biomedical and molecular biology applications.[6] Therefore, the gold nanoparticles growth needs to be controlled in order to make use of different properties that appear as we change their size and shape. Gold nanoparticles are generally prepared by chemical reduction of an appropriate gold precursor, usually $HAuCl_4$ with reducing agents including organic acid, alcohols and others. The shape and size of gold nanoparticles are determined by numerous factors; these include the selecting the reactant concentrations, temperature, pH, additives as well as the surfactant.

Since size-depending optical spectra of nanoparticles can be easily obtained by chromatographic systems with diode array detection,[7,8] as well as UV detection based on light scattering,[9] chromatographic methods can be easily utilized for the characterization of size-dependent properties of metal as well as non-metal nanoparticles. It should be noted that the surface area and particle size of the column material are important factors of the adsorption process,[10] and the adsorption of gold nanoparticles onto the surface of functionalized silica has been demonstrated.[11]

In our previous work, silica colloids with 78, 28 and 11 nm were separated in size-exclusion chromatography (SEC) in 100 min[9] as well as by hydrodynamic chromatography (HDC) using a nonporous silica-packed column.[12] We found that the latter method could have the potential of achieving a higher separation efficiency of these colloids by using packing particles of 1.9 μm or smaller diameter. However, due to the high back pressure of the system, the use of smaller nonporous silica is limited. In order to overcome this drawback, we fabricated monolithic silica capillary columns with a diameter of 50 μm, in which the silica backbone was designed so that it could produce many "micro-channels" (formed by the through-pore along the column). Sakai-Kato *et al*. have recently reported on the size-based separation of silica nanoparticles using monolithic capillary columns.[13]

Monolithic capillary columns are alternative to traditional particulate solid phases, and have been used for various applications in gas or liquid chromatography (LC) for a long time. The advantages of capillary columns in LC are attributed

† To whom correspondence should be addressed.
E-mail: take-t@gifu-u.ac.jp

to the narrow column diameter and the low eluent flow rate. The high efficiency and resolution of monolithic columns have been reported for some applications in the last ten years.[14-16] It is natural to recognize that capillary LC saves solvents, reagents and it is quite friendly to the environment. Monolithic columns are extremely permeable, and offer a high efficiency that slowly decreases with increasing flow velocity.[17,18] At present, monolithic silica capillary columns can be one of the most prospective separation media due to mechanical stability, column efficiency and permeability.[19] Monolithic silica capillary columns were selected in this study because the efficiency of the silica is higher compared to polymer monolithic capillary columns. Silica also has greater mechanical stability, because it does not swell or shrink.[19] In this study we investigate the separation of gold nanoparticles on monolithic silica columns in LC.

Experimental

Apparatus

The system used in this work consisted of a capillary LC system constructed by an L.TEX-8301 Micro Feeder (L.TEX Corp., Tokyo, Japan) equipped with an MS-GAN 050 gas-tight syringe (0.5 mL; Ito, Fuji, Japan) as a pump, a Model CN4-4344.02 microinjection valve with an injection volume of 20 nL (Valco, Houston, TX) as an injector, a laboratory-made monolithic silica capillary column (200 – 2000 mm × 0.050 mm i.d.) and a CE-1570 UV-VIS detector (JASCO, Tokyo, Japan). The UV detector was operated at 530 nm, and samples were visualized by on-column detection. The data were acquired by a Chromatopac C-R4A data processor (Shimadzu, Kyoto, Japan). UV-VIS absorption spectra of gold nanoparticles were measured by a U-4100 UV-VIS spectrophotometer (Hitachi, Tokyo, Japan). The size and morphology of gold nanoparticles were examined by a transmission electron microscope (JEM 2100; JEOL, Tokyo, Japan). The particle size and size distribution were characterized by dynamic light scattering (DLS-7000L; Photal Otsuka Electronics, Osaka, Japan).

Reagents and materials

The reagents were obtained from Wako Pure Chemical Industries (Osaka, Japan), and used as received. Tetramethoxysilane (TMOS) was purchased from Tokyo Chemical Industry (Tokyo, Japan). PEG 10000 (M_W = 10000) was purchased from Sigma-Aldrich Japan (Tokyo, Japan). Purified water was produced in the laboratory by using an RFU 424 CA ultrapure water system (Advantec, Tokyo, Japan). $HAuCl_4 \cdot 4H_2O$ was of analytically pure grade and used without further purification.

Preparations of gold particles

Gold nanoparticles were synthesized by the reduction of $HAuCl_4$ as gold precursor with reducing agents, such as sodium citrate, as reported by Doron *et al*.[20] A 50 – 400 µL volume of 1% (w/w) $HAuCl_4$ solution was added to 10 mL distilled water and heated to the boiling point under stirring condition. Then, 250 µL of a 1% (w/w) sodium citrate solution was added to the boiling solution instantly, and the pale-yellow color of the solution was gradually darkened to purple, and finally turned to deep wine red. The wine-red solution showed that the gold nanoparticles were formed. All colloids were stored at room temperature and were generally used within 1 month after preparation. In addition, the nucleation time was measured by using a stop watch.

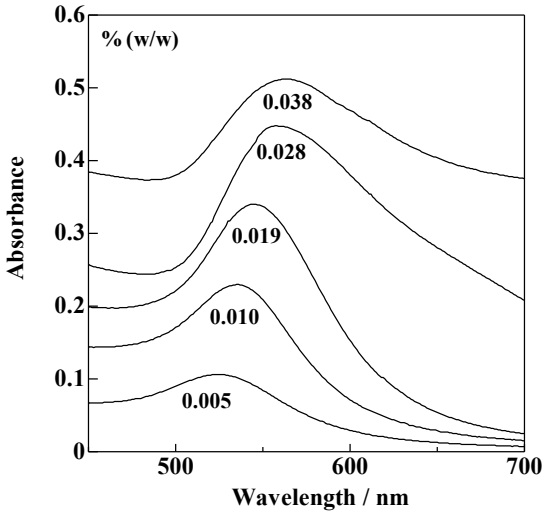

Fig. 1 UV-VIS spectra of gold nanoparticles for various volumes of $HAuCl_4$.

Preparation of monolithic capillary column

Monolithic capillary columns (200 – 2000 × 0.050 mm i.d.) were prepared *via* the *in-situ* sol-gel process in a manner similar to our previous report,[21] with some modifications to the preparation conditions; 2.0 mL of TMOS together with 0.53 g PEG 10000 were dissolved in 5.0 mL of 0.01 M acetic acid by stirring the solution for 30 min at 0°C. The solution was filled into pretreated fused-silica capillaries. After leaving the capillaries at 40°C for 24 h, they were washed with 60% ethanol, and heated at 330°C for 3 h, followed by purging with nitrogen gas at 110°C for 1 h. After that, they were washed with toluene, THF, methanol and the eluent prior to use. The process for growing mesopores was skipped because mesopore-less monoliths were preferred in the present work. To compare the result in this study, 1.9-µm nonporous silica packed columns and monolithic columns with normal mesopore sizes were also prepared. Mesopore could be grown by filling monolithic capillary columns with a 0.1 M ammonia aqueous solution and kept at 60°C for 45 h just after gelation.

Results and Discussion

UV-VIS spectra and color of gold nanoparticles

UV-VIS spectra were obtained using prism-grating monochromators with a 10-mm rectangular cell holder for the sample compartment. Absorbance measurements were made over the wavelength range of 200 – 800 nm. Figure 1 demonstrates spectra of gold nanoparticles prepared under different conditions in the visible wavelength region. It can be seen that as the concentration of $HAuCl_4$ increases, the maximum absorption wavelength increases. The absorption wavelength depends on the shape and size of the particles, *i.e*. larger particles and more unsymmetrical particles absorbing at longer wavelengths than smaller and more spherical particles.[22] We could therefore conclude that the size of the gold nanoparticles increases with increasing concentration of $HAuCl_4$. A higher absorbance was observed for larger concentrations. The above result could be explained by the fact that light is an electromagnetic wave which produces forces on electrons for moving faster. Since the wave is oscillating,

the speeding up of charges is oscillatory. Metals have conduction electrons that are comparatively free to move. Therefore, an electronic wave will cause them to oscillate. When gold nanoparticles are irradiated by light, the electric field of the light waves induces coherent oscillation of the free electrons, known as surface plasmon resonance (SPR). The SPR depends on the shape and size of the particles.[23] Larger particles absorb visible light at longer wavelengths than smaller particles. The SPR is clearly visible with increasing particle diameter (the maximum absorption wavelength of the gold colloid increased, *e.g.*, 523 to 560 nm as the concentration of $HAuCl_4$ increased from 0.005 to 0.038% (w/w). In addition, nanoparticles also absorb selected portions of the visible light, for example, the gold-nanoparticle solutions mentioned above are red, which strongly absorb light at 520 – 560 nm (green). The red-purple color of the solution resulted from the fact that the green components of white light were removed.

Table 1 Effect of $HAuCl_4$ concentration on the nucleation time as well as mean particle size

Concentration of $HAuCl_4$, % (w/w)	Approximate time for nucleation/s	Mean particle size/ nm
0.005	120	13 ± 2.5
0.010	90	17 ± 2.7
0.019	60	33 ± 5.2
0.028	30	43 ± 5.1
0.038	25	61 ± 5.6

Size distribution of gold nanoparticles

Dynamic light scattering (DLS) is an analytical tool widely used to determine the average particle diameter of suspending nanoparticles or polymers in solution. Table 1 summarizes the

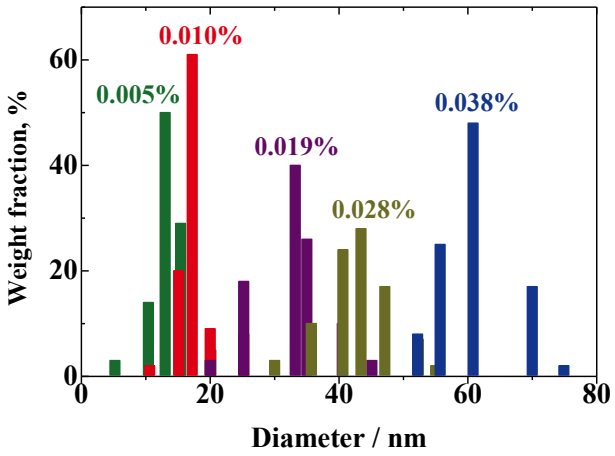

Fig. 2 Size distribution of gold nanoparticles by DLS.

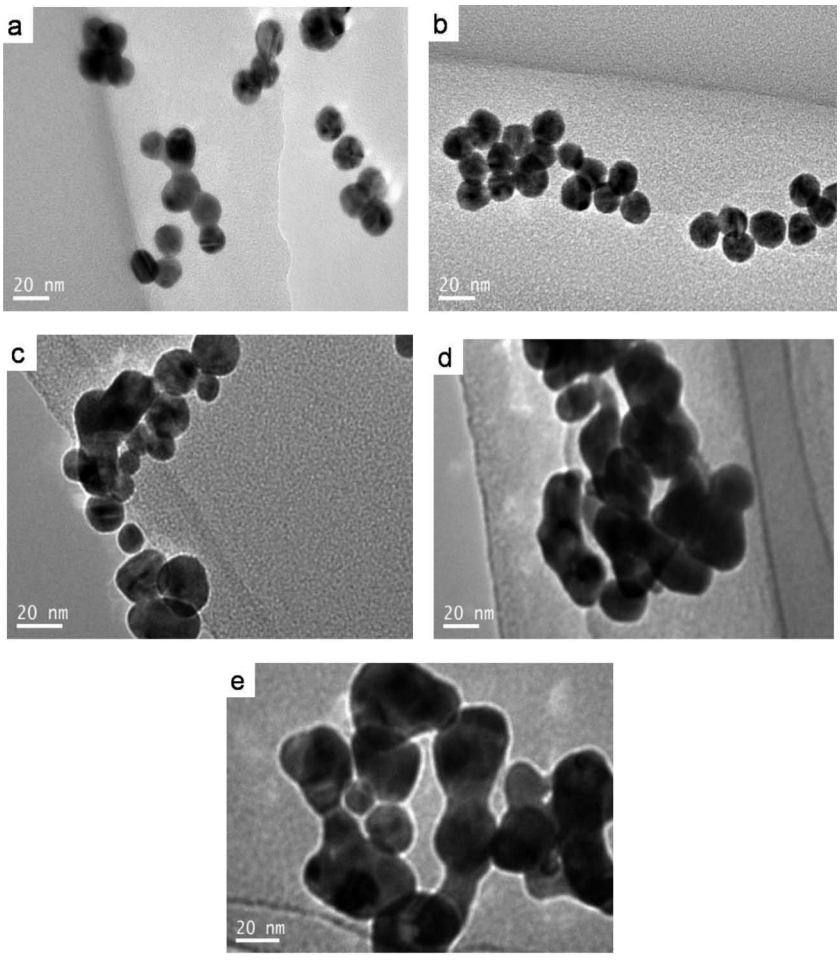

Fig. 3 TEM images of gold nanoparticles: (a) 13, (b) 17, (c) 33, (d) 43, (e) 61 nm.

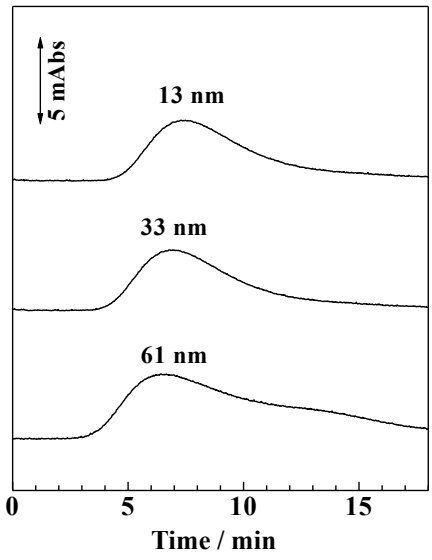

Fig. 4 Elution profiles of gold nanoparticles for water as the mobile phase. Column, monolith (200 × 0.050 mm i.d.); mobile phase, water; analytes, 13, 33 or 61-nm gold nanoparticles; sample volume, 20 nL; flow rate, 0.1 μL/min; wavelength of detection, 530 nm.

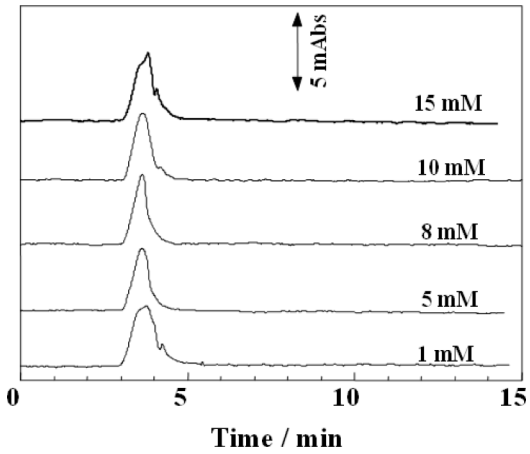

Fig. 5 Elution profiles of gold nanoparticles for aqueous SDS solution as the mobile phase. Mobile phase, aqueous SDS solution with different concentrations as indicated; analytes, 61 nm gold nanoparticle; other operating conditions were the same as in Fig. 4.

result of the DLS measurement. It can be seen that the 0.005% (w/w) $HAuCl_4$ had a complete nucleation time of 120 s with an average particle size of (13 ± 2.5) nm. With increasing concentration of $HAuCl_4$, the mean particles diameter also increased from 13 to 61 nm. Gold nanoparticles with sizes of (13 ± 2.5) and (17 ± 2.7) nm have narrower size distributions, and thus possess more uniform size than the others. Figure 2 shows the size distribution by DLS in a histogram for gold nanoparticles prepared under different $HAuCl_4$ concentrations. It can be seen that the diameter size of gold nanoparticles increases with increasing concentration of $HAuCl_4$. These results indicate that an additional supply of $HAuCl_4$ makes the gold particles grow further.

TEM images of gold nanoparticles

The size and shape of nanoparticles can be measured by several techniques, such as atomic force microscopy, small-angle X-ray scattering, X-ray diffraction and transmission electron microscopy (TEM).[24] In this study, TEM was used to determine the size and shape of the synthesized gold nanoparticles, and the TEM images in Fig. 3 show that each solution contains a variety of the size and the shape; gold nanoparticles with (13 ± 2.5) and (17 ± 2.7) nm diameters are illustrated as being almost symmetric and spherical, while the larger gold nanoparticles are slightly nonuniform and less spherical. Larger sizes of gold nanoparticles were formed by increasing the concentration of $HAuCl_4$. However, it was noticed that the nucleation time was gradually decreased. Due to the rapid nucleation time, the formation of gold nanoparticles with less uniform particle (less spherical in shape) was observed.

Elution profile of gold nanoparticles and the effect of surfactant

The elution of the gold nanoparticles was first carried out using pure water as the elution solvent, as demonstrated in Fig. 4. The results show that the elution profiles of the gold nanoparticles were severely broadened by using water alone. This could be due to agglomeration of the nanoparticles in water. In order to overcome these drawbacks, we added SDS to the eluent. Surfactants are usually amphiphilic compounds that contain a hydrophobic tail and a hydrophilic head. The association of surfactants with particles stabilizes them by an electrostatic or steric effect to prevent further agglomeration of the particles;[25] this effect of the surfactant was crucial in our study. The gold nanoparticles are expected to be capped with citrate ions. The interaction between hydrophobic tails of SDS and the gold surface causes the adsorption of SDS onto the surfaces of the nanoparticles. This process results in an exchange from citrate to SDS of the stabilizing reagent on the gold nanoparticles.[26] Different concentrations of SDS were examined in this study to obtain the optimum condition so that gold nanoparticles sample would not coagulate during chromatographic separation. The effect of the concentration of SDS solutions in the mobile phase on the peak shape was examined; the results are shown in Fig. 5. It can be seen that the elution profiles were slightly different at different SDS concentrations. At lower and higher SDS concentrations, the peak was slightly broader and composed of more than one peak signal, while the best peak shape was observed at around 8 mM, *i.e*. the critical micelle concentration (CMC) of SDS. When the SDS concentration was higher than CMC, slightly unstable baseline and broadened peaks were observed in Fig. 5. From these results, 8 mM of aqueous SDS solution was selected in this study.

Separation of gold nanoparticles

Figure 6a demonstrates the elution of gold nanoparticles using a monolithic silica capillary column with 400 × 0.050 mm i.d. at a flow rate of 0.1 μL/min, whereas Fig. 6b shows the size of gold nanoparticles as a function of the elution times. It can be seen that the smaller size of gold nanoparticles, a larger elution time is observed. Since the empty volume of the capillary column employed is calculated to be 0.79 μL, the interstitial volume should be smaller than 0.79 μL due to the monolith skeleton. For example, it is at most 0.63 μL, assuming that 80% of the inner volume is available for the nanoparticles. In addition, since the monolith was directly connected to the injector and the on-column detection was adopted, the dead volume can be expected to be almost zero in this study. It is found from Fig. 6 that the gold nanoparticles were eluted after 6.3 min, which means that the nanoparticles were retained by

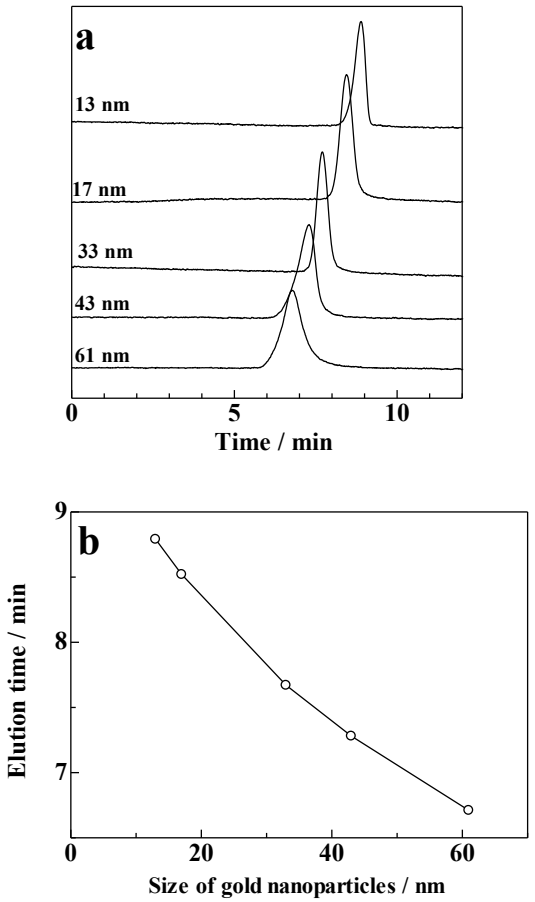

Fig. 6 Elution profiles of gold nanoparticles with different sizes (a), and the elution time as a function of the gold nanoparticle size (b). Column, monolith (400 × 0.050 mm i.d.); sample volume, 20 nL; wavelength of detection, 530 nm; mobile phase, 8 mM SDS; flow rate, 0.1 μL/min.

adsorption on the silica surface. When these nanoparticles elute in the HDC mode without any interaction with the silica surface, they should elute before the time corresponding to the interstitial volume. Considering these results, it is expected that the gold nanoparticles can be separated by the adsorption mode, although the exclusion effect based on the size effect may be involved. It is reasonable to expect that larger particles have less chance to contact the silica surface, leading to less retention. Since the process of growing mesopores was skipped, it is expected that the size of mesopores is smaller than 10 nm to the best of our knowledge. Therefore, the permeation of gold nanoparticles investigated in the present work into the mesopores can also be neglected. The separations of gold nanoparticles mixtures are demonstrated in Fig. 7, where a monolithic silica capillary (400 × 0.050 mm i.d.) was used as the separation media and 8 mM SDS aqueous solution was used as the mobile phase, and the flow rate was 0.1 μL/min with the sample volume of 20 nL. The UV detector was operated at 530 nm. The mixture of gold nanoparticles with 61 and 43 nm average sizes eluted closely together, and nearly the same result was observed for a mixture of 61 and 33 nm. Contrarily, mixtures of 61 and 13 nm as well as 61 and 17 nm could be partially separated.

Comparison with other types of columns

Chromatograms obtained using monolith columns with different mesopore growing steps are shown in Fig. 8. From

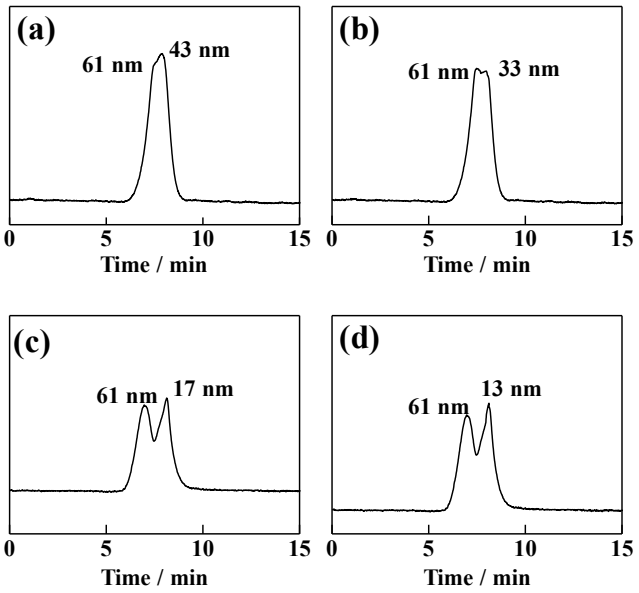

Fig. 7 Separation of gold nanoparticle mixtures on a 400-mm column. Samples, 43 and 61 nm for (a), 33 and 61 nm for (b), 17 and 61 nm for (c), 13 and 61 nm for (d), other operating conditions were the same as in Fig. 6.

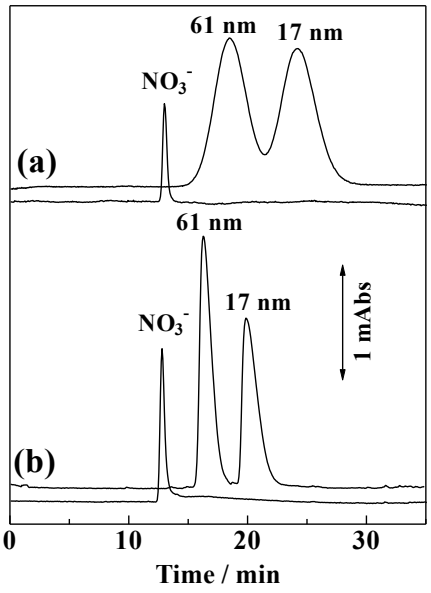

Fig. 8 Separation of gold nanoparticle mixtures on monolith columns with different mesopore growing steps. Columns, monolith with a mesopore growing step (a) or without any mesopore growing step (b), 1000 × 0.050 mm i.d.; analytes, gold nanoparticles for the upper trace and 1 mM sodium nitrate for the lower trace; other conditions were the same as in Fig. 6.

Fig. 8, it can be seen that better resolution of gold nanoparticles was achieved on the mesopore-less monolithic column. It is probable that slow diffusion in the mesopore leads to band broadening. Under these conditions, the obtained selectivity (separation factor) was 2.24 for the mesopore-less monolithic column, whereas 1.98 for the monolithic column with a mesopore growing step. The largest selectivity (separation factor) was obtained for the mesopore-less monolithic column

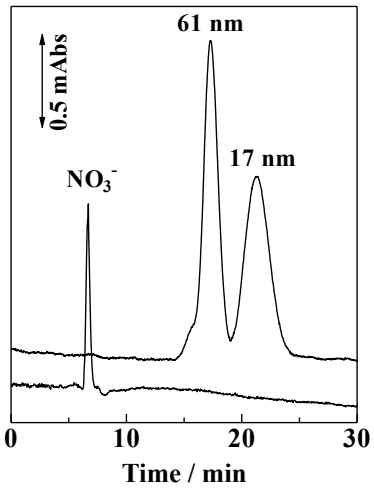

Fig. 9 Separation of gold nanoparticle mixtures on a packed column. Column, Hipresica FQ N2N (1.9 μm, 100 × 0.32 mm i.d.); analyte, 61 and 17 nm; sample volume, 0.2 μL; wavelength of detection, 530 nm; mobile phase, 8 mM SDS; flow rate, 0.5 μL/min; analytes, gold nanoparticles for the upper trace and 1 mM sodium nitrate for the lower trace.

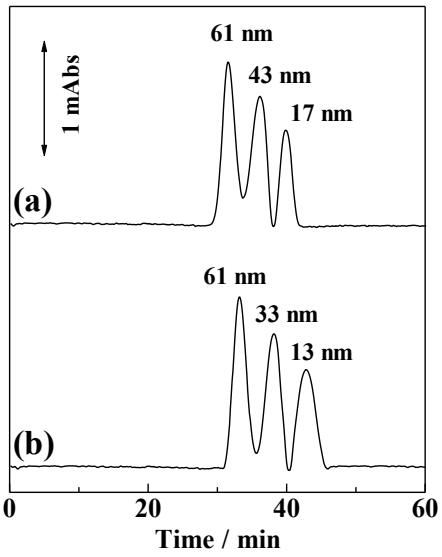

Fig. 10 Separation of gold nanoparticle mixtures on a 2000-mm column. Column, monolith (2000 × 0.050 mm i.d.); analytes, 61, 43 and 17 nm (a) and 61, 33 and 13 nm (b); other conditions were the same as in Fig. 6.

among the columns examined.

A comparison with another type of column is the way to prove the columns that we used were optimum. We used packed columns and monolithic columns with different mesopore growing steps. Figure 9 shows the separation of gold nanoparticles 61 and 17 nm on a 1.9-μm nonporous silica packed column. It can be seen that two gold nanoparticles are separated, and the better resolution was obtained at the sacrifice of the analysis time, compared with Fig. 7C. The selectivity (separation factor) obtained in Fig. 9 was 1.38. In addition, the selectivity (separation factor) was calculated assuming that nitrate was a non-retained analyte

Figures 8 and 9 also show elution profiles for sodium nitrate, which is expected to elute without any interaction with the silica surface. It can be seen that sodium nitrate elutes faster than gold nanoparticles. This indicates that gold nanoparticles are retained on the silica surfaces.

Use of a longer column also improved the resolution, as demonstrated in Fig. 10. The resolution of gold nanoparticles was improved by using a 2000-mm column, although it took a longer elution time. The repeatability for the elution time, peak area and peak height of gold nanoparticles with 61, 33 and 13 nm diameters were examined for five successive measurements under the conditions in Fig. 10, as shown in Table 2. It can be seen that the relative standard deviation (RSD) values were less than 0.95% for the elution time, whereas those for the peak area and the peak height were less than 3.6%.

Table 2 Repeatability of the elution time, peak area and peak height for 61, 33 and 13 nm

	RSD, % (n = 5)		
	61 nm	33 nm	13 nm
Elution time	0.94	0.93	0.95
Peak area	3.4	3.5	3.6
Peak height	2.2	2.1	2.0

Column, monolith (2000 × 0.050 mm i.d.); sample volume, 20 nL; wavelength of detection, 530 nm; mobile phase, 8 mM SDS; flow rate, 0.1 μL/min.

Conclusions

Gold nanoparticles with the mean particle size ranging from 13 to 61 nm were prepared by the reduction of $HAuCl_4$ with sodium citrate. The size of the gold nanoparticles could be varied by changing the $HAuCl_4$ concentration. The gold nanoparticles prepared were analyzed by UV-VIS, DLS and TEM. The use of surfactants as the mobile phase was effective to improve the elution profiles of gold nanoparticles. An aqueous solution of 8 mM of SDS was optimum for the separation of gold nanoparticles on monolithic silica capillary columns with 0.050 mm i.d. The resolution of gold nanoparticles was improved by increasing the length of the separation column. Gold nanoparticles were retained on silica columns by adsorption. Better resolution was achieved using a monolithic column mesopore-less than the use of a nonporous silica packed column or a monolithic column with a mesopore growing step. The proposed separation method would serve as an alternative to SEC as well as FFF for the separation of metallic nanoparticles due to its simple separation mechanism.

Acknowledgements

The authors are grateful for partial financial support from the Gifu University Young Researchers Education Centers for Innovation, Japan.

References

1. P. Mulvaney, *Langmuir*, **1996**, *12*, 788.
2. X. Huang, I. H. El-Sayed, H. Ivan, X. Yi, and M. A. El-Sayed, *J. Photochem. Photobiol., B*, **2005**, *81*, 76.

3. S. Tedesco, H. Doyle, J. Blasco, G. Redmond, and D. Sheehan, *Aquat. Toxicol*., **2010**, *100*, 178.
4. X. Qian and H. S. Park, *J. Mech. Phys. Solids*, **2010**, *58*, 330.
5. D. V. Goia and E. Matijević, *Colloids Surf., A*, **1999**, *146*, 139.
6. W. Lu, W. Wang, Y. Su, J. Li, and L. Jiang, *Nanotechnology*, **2005**, *16*, 2582.
7. K. A. Littau, P. J. Szajowski, A. J. Muller, A. R. Kortan, and L. E. Brus, *J. Phys. Chem*., **1993**, *97*, 1224.
8. R. W. Devenish, T. Goulding, B. T. Heaton, and R. Whyman, *J. Chem. Soc., Dalton Trans*., **1996**, 673.
9. Z. Aspanut, T. Yamada, L. W. Lim, and T. Takeuchi, *Anal. Bioanal. Chem*., **2008**, *391*, 353.
10. S. J. Gregg and K. S. W. Sing, "*Adsorption, Surface Area and Porosity*", 2nd ed., **1982**, Academic Press Inc., London, New York.
11. S. L. Westcott, S. J. Oldenburg, J. Steven, T. R. Lee, and N. J. Halas, *Langmuir*, **1998**, *14*, 5396.
12. T. Takeuchi, Siswoyo, Z. Aspanut, and L. W. Lim, *Anal. Sci*., **2009**, *25*, 301.
13. K. Sakai-Kato, S. Ota, T. Takeuchi, and T. Kawanishi, *J. Chromatogr., A*, **2011**, *1218*, 5520.
14. V. V. Tolstikov, A. Lommen, K. Nakanishi, N. Tanaka, and O. Fiehn, *Anal. Chem*., **2003**, *75*, 6737.
15. K. W. Ro, J. Liu, M. Busman, and D. R. Knapp, *J. Chromatogr., A*, **2004**, *1047*, 49.
16. O. Nunez, T. Ikegami, K. Miyamoto, and N. Tanaka, *J. Chromatogr., A*, **2007**, *1175*, 7.
17. T. Takeuchi, *Anal. Bioanal. Chem*., **2003**, *375*, 25.
18. G. Guiochon, *J. Chromatogr., A*, **2007**, *1168*, 101.
19. N. Tanaka, H. Kobayashi, K. Nakanishi, H. Minakuchi, and N. Ishizuka, *Anal. Chem*., **2001**, *73*, 420A.
20. A. Doron, E. Katz, and I. Willner, *Langmuir*, **1995**, *11*, 1313.
21. L. W. Lim, K. Hirose, S. Tatsumi, H. Uzu, M. Mizukami, and T. Takeuchi, *J. Chromatogr., A*, **2004**, *1033*, 205.
22. I. Uechi and S. Yamada, *Anal. Bioanal. Chem*., **2008**, *391*, 2411.
23. K. L. Kelly, E. Coronado, L. L. Zhao, and G. C. Schatz, *J. Phys. Chem. B*, **2003**, *107*, 668.
24. A. C. Templeton, W. P. Wuelfing, and R. W. Murray, *Acc. Chem. Res*., **2000**, *33*, 27.
25. G.-T. Wei and F.-K. Liu, *J. Chromatogr., A*, **1999**, *836*, 253.
26. F.-K. Liu and G.-T. Wei, *Anal. Chim. Acta*, **2004**, *510*, 77.